

THE RFZ/RPG APPROACH TO CONTROL
ROOM MONITORING

2157 (I-6)

Peter D'Antonio and John H. Konnert
RPG Diffusor Systems, Inc.
Largo, Maryland

**Presented at
the 76th Convention
1984 October 8-11
New York**



AES

This preprint has been reproduced from the author's advance manuscript, without editing, corrections or consideration by the Review Board. The AES takes no responsibility for the contents.

Additional preprints may be obtained by sending request and remittance to the Audio Engineering Society, 60 East 42nd Street, New York, New York 10165 USA.

All rights reserved. Reproduction of this preprint, or any portion thereof, is not permitted without direct permission from the Journal of the Audio Engineering Society.

AN AUDIO ENGINEERING SOCIETY PREPRINT

THE RFZ/RPG APPROACH TO CONTROL ROOM MONITORING

by PETER D'ANTONIO and JOHN H. KONNERT

RPG DIFFUSOR SYSTEMS, INC.
12003 Wimbledon St.
Largo, MD 20772

A design for implementing a LEDE control room is proposed. The dead end is achieved by creating an RFZ by flush mounting the monitors as close to a trihedral corner as is physically possible and splaying the absorbent side walls and ceiling to minimize interfering reflections at the mix position. The live end is achieved by positioning RPG diffusers \blacksquare the rear wall in such a manner as to reintroduce the energy passing the mix position, after an initial time delay, temporally and spatially diffused. The approach leads to accurate monitoring, with a stereo image which is maintained across the entire width of the console and in the rear of the room.

0 INTRODUCTION

We would like to address only two of the many aspects of control room design—namely, the boundary surfaces in the front half of the room, which surround the monitor speakers, and those in the rear half of the room. The proposal is essentially an implementation of the LEDE¹ approach, which utilizes a reflection free zone, RFZ, in the front of the control room and a reflection phase grating, RPG², diffuse sound field in the rear of the room.

The placement of a low frequency source relative to rigid, massive boundaries is of critical importance in determining the frequency spectrum perceived. This is because both constructive and destructive interference occurs among the spectra from the main source and the reflections. A method has been presented by Berger[1] to approximate the overall Speaker/Boundary Interference Response (SBIR). A method is discussed here that addresses the positional dependence of the observer by computing the frequency response perceived at any location. This is accomplished by treating every wall reflection as arising from a virtual source on the opposite side of the reflecting surface. A virtual source is graphically located an equal distance across a reflecting boundary on a line perpendicular to that boundary. Each boundary that is crossed causes a change in the sign of the coordinate which is perpendicular to the boundary. For example, in Figure 1 a point source (dot) at position (x,y,z) with respect to the trihedral corner origin $x=y=z=0$, and the three virtual sources (cross), arising from the $x=0$ and $y=0$ boundaries at $(x,-y,z)$, $(-x,-y,z)$ and $(-x,y,z)$, are shown. The additional four virtual sources (circle)

¹LEDE is a registered trademark of Synergetic Audio Concepts

²RPG and QRD are registered trademarks of RRG Diffusor Systems, Inc.

generated by the $z=0$ boundary are also shown at $[x,y,-z]$, $[x,-y,-z]$. We thus have the eight sources to consider. Fresnel diffraction from all these sources yields their combined, coherently summed amplitude, A , for any observation point (x_o, y_o, z_o) .

$$|A|_{x_o y_o z_o} = \left| \sum_{p=1}^8 a_p \exp(2\pi i d_p / \lambda) / d_p \right| \quad (1)$$

where d_p is the distance from source p to the point of observation and a_p represents the reflection efficiency. The source with one negative coordinate represents single reflections, those with two negative coordinates represent double reflections, and $(-x,-y,-z)$ represents the source for triple reflections. It is interesting to note that the $(-x,-y,-z)$ source is the one utilized in reflecting "corner cubes". These were used to reflect a laser signal back to earth from the surface of the moon and are also used in highway reflectors, since they reflect a signal back in the direction of incidence.

For similar boundaries, the coefficients a_p for the triple reflection source will be the cube of that for single reflections, and that for double reflections will be the square. The coefficients could be frequency dependent, i.e. absorption coefficients, and could also be complex, to account for a phase shift at a boundary or other real sources in a multiple driver speaker. The presence of only one or two boundaries, rather than three, may be easily treated by including only those terms in Eq. 1 for the appropriate boundaries.

As an example we will consider a room with a 10 foot ceiling and a speaker near a trihedral corner ($x=y=z=0$), 2 feet from the ceiling and 2 feet from each of the walls ($x=y=z=2$ feet). The geometry is shown in Figure 2. The interference patterns calculated at the observation coordinates $(5.0, 8.66, 6.0)$, indicated by the dashed line, and $(1.0, 8.66, 6.0)$, indicated by the long-short dashed line, are shown. Since the surfaces are reflective, $a_p=1$, severe comb filtering, which is position dependent, is observed.

1 FAR-FIELD APPROXIMATION

How does the far-field response compare with the near-field? The far-field response is valid when the distances of the source from the trihedral walls are much less than the distance from the corner to the observer. This condition will generally not be satisfied in a control room. However, it can be used as an overall guide to the spectra of the room. This is what Berger[1] has examined. It is of interest to derive the far-field expression and compare the near and far-field results.

In the far-field, Eq. 1 becomes

$$A_m = \sum_{p=1}^8 a_p \exp(is \cdot r_p) \quad (2)$$

where r_p is the vector from the origin of the coordinate system to source p , $s=4\pi \cdot u/\lambda$, and u is a unit vector in the direction of interest. the intensity is given by

$$|A|_m^2 = A_m \cdot A_m^* \quad (3)$$

where * represents the complex conjugate operation.

$$|A|_m^2 = \left[\sum_{p=1}^8 a_p \exp(is \cdot r_p) \right] \left[\sum_{q=1}^8 a_q \exp(is \cdot r_q) \right] \quad (4)$$

Each of the double summations is taken from 1 to 8, where 8 is the total number of sources for the trihedral condition. There will be 8 terms for which $p=q$ and $r_p=r_q$. For each of these the exponential factor is unity. There remain $8(8-1)$ or 56 terms for which p does not equal q . For these terms, r_p-r_q represents the vector distance between source p and q . Eq. 4 can be rearranged to give

$$|A|_m^2 = \sum_{p=1}^8 a_p^2 + 2 \sum_{p=1}^8 a_p a_q \cos s \cdot (r_p - r_q) \quad (5)$$

The two terms in the double sum involving sources p and q together become $2a_p a_q \cos[s \cdot (r_p - r_q)]$ due to the equality $2\cos[s \cdot (r_p - r_q)] = \exp[is \cdot (r_p - r_q)] + \exp[-is \cdot (r_p - r_q)]$ (6)

Reference to Figure 1 indicates the multiplicity of the inter-source vectors. To obtain the far-field expression we must integrate over all scattering vector directions. We are interested in only an octant, but the mmm symmetry (three perpendicular mirror planes) of Figure 1 indicates the total scattering into each octant is the same. If we set all $a_p=1$ and integrate over all the scattering directions (see for example p. 466, James [2]), we obtain

$$\begin{aligned} |A|_m^2 \sim & 8 + 8\sin(4\pi(x/\lambda))/4\pi(x/\lambda) + 8\sin(4\pi(y/\lambda))/4\pi(y/\lambda) \\ & + 8\sin(4\pi(z/\lambda))/4\pi(z/\lambda) + 8\sin[4\pi(x^2+y^2)^{1/2}/\lambda]/4\pi(x^2+y^2)^{1/2}/\lambda \\ & + 8\sin[4\pi(x^2+z^2)^{1/2}/\lambda]/4\pi(x^2+z^2)^{1/2}/\lambda \\ & + 8\sin[4\pi(y^2+z^2)^{1/2}/\lambda]/4\pi(y^2+z^2)^{1/2}/\lambda \\ & + 8\sin[4\pi(x^2+y^2+z^2)^{1/2}/\lambda]/4\pi(x^2+y^2+z^2)^{1/2}/\lambda \quad (7) \end{aligned}$$

This is the formula evaluated by Berger [1] for the three boundary condition. For two boundaries this reduces to

$$|A|_{\text{max}}^2 \sim 4 + 4\sin(4\pi y/\lambda)/4\pi y/\lambda \\ 4\sin[4\pi(x^2+y^2)^{1/2}/\lambda]/4\pi(x^2+y^2)^{1/2}/\lambda \quad (8)$$

For one boundary

$$|A|_{\text{max}}^2 \sim 2 + 2\sin(4\pi x/\lambda)/4\pi x/\lambda \quad (9)$$

Converting to dB, we obtain a 6 dB increase for one boundary, 12 dB increase for two and an 18 dB increase for three boundaries over the free field situation if we set the function $\sin x/x$ equal to its maximum value of 1.

In Figure 2 (solid line) we see the far-field intensity for the trihedral case with $x=y=z=2$ feet calculated earlier with the near-field theory. The first minimum occurs at approximately 400 Hz, as it did in the near-field calculation close to the left wall. The energy is 21 dB down as compared to 28 dB for the near-field calculation. It can be seen that the far-field integration has averaged the response at frequencies above the first minimum. Just as Eq. 7, 8 and 9 are far-field approximations, Eq. 1 is a near-field approximation, which assumes infinitely extending wall segments. They are limiting cases, and it can be shown that as the observation distance becomes very large Eq. 1 yields the response predicted by Eqs. 7, 8, and 9. Clearly a much more elaborate calculation, which will be discussed in a future paper, is required in which the amplitude and phase of each point on each finite boundary surface is coherently summed. The main point to be realized at this time, is that the first interference minimum occurs at higher frequencies as the source approaches the trihedral corner. That is, a point source located in the trihedral corner will have ideally a flat SBIR at some observation point, because the observation point is in an RFZ, since there are no interfering reflections from the boundary surfaces. It seems prudent, therefore, to try to locate the woofer in a large multiple-driver speaker cabinet as close to the trihedral corner as is physically possible and splay the boundaries such that an RFZ is realized over a rather wide volume, which extends across the entire mixing console, several feet above, and far enough in back to allow for a producer area behind the mix position.

2 CONTROL ROOM DESIGN-RFZ

The key point which follows from these calculations and LEDE¹ precepts [3] is that the objective for the front of the control room is to generate an RFZ where the predominant energy is from the monitor speakers. In terms of the virtual image construct we want to decrease the contribution of the virtual images at the mix position, either by reducing the number of sources by baffling and splaying of the boundary surfaces or by reducing the coefficients, a_p , by applying absorptive material to the boundary surfaces. At some frequency, depending on the boundary sizes, the reflections will begin to depart from purely specular behavior and there may be significant energy in non-specular

directions. Because of this both reflection control and absorption are useful.

Consider the geometry in Figure 3, in which the side walls are splayed 120° with respect to the front wall. It can be seen that the virtual sources present in the orthogonal case in Figure 1 at $(-x,-y,z)$ and $(-x,-y,-z)$, arising from double and triple reflections, are not present. We have reduced the number of sources from 8 to 6. If in addition to splaying the side walls, the monitors are flush mounted in rigid, massive baffles, with the acoustic center of the woofer positioned on the 120° angle bisector, the $(x,-y,z)$ and $(-x,y,z)$ sources are obscured from contributing at the mix position and an RFZ is created. The RFZ is indicated in Figure 3 by the area within the dashed lines. The position of the virtual sources arising from the side walls and the width of the speaker baffle essentially define a phantom source. One can optimize the size of the speaker baffle to either decrease or increase the RFZ. The position in Figure 3 was chosen to provide an RFZ across the width of the console which is shown. All surfaces in the dead front end (DE) are absorptive. If the speakers are located along side the window, rather than above, then window reflections are minimized in the RFZ. The window should be tilted downward to minimize the contribution of energy arriving from the rear at the mix position. Since the energy returning from the rear of the room is uniformly diffused and lower in level, this interference is minimized. The mix position is the small cross near the console located on the live-end (LE) dead-end (DE) or LEDE dashed line. The axes of the high frequency sources are oriented toward the asterisk a foot or so behind the mix position.

The speaker baffle is inclined such that the axis of the high frequency driver, the long-short dash line, is focused a foot or so behind the LEDE verticle dashed line, shown in Figure 4. The $(x,y,-z)$, $(-x,y,-z)$ and $(x,-y,-z)$ sources can likewise be minimized by utilizing a trapezoidal rigid, massive baffle sloping forward from the top of the speaker to the ceiling, as indicated in Figure 4. The angle this boundary makes with the speaker baffle and sloping ceiling is determined by the location of the intersection of the dotted lines arising from virtual sources of the woofer, the upper dot, with respect to the trapezoidal baffle and rising ceiling. This point is shown as the intersection of the virtual source dotted lines, which represent the lowest reflections of the woofer from the trapezoidal baffle and rising ceiling. In the geometry of Figure 4, the RFZ extends approximately four feet above the mix position and six feet behind. The woofer will also reflect off the surface below the speaker baffle out to the dotted line shown, and consequently a substantial amount of low frequency absorption in this area will be useful.

3 CONTROL ROOM DESIGN-RPG

The energy which crosses the LEDE plane and returns from the rear wall is a constant, ignoring absorption, regardless what surface treatment or geometry is used for the rear half of the room. What is important, is the temporal and spatial distribution of energy in this plane or

more importantly, in the section of this plane where the mixer is apt to be. The diffuse energy should arrive back at the mix position after an initial time delay, spread in time and spatially distributed across the entire width of the mixing console. The importance of the initial time delay to the perceived size of a room has been well documented [3,4]. The rear surfaces should be arranged such that the temporally and spatially diffuse energy arrives within the temporal fusion zone, where the diffuse energy from the rear wall is blended with the direct sound, increasing the intensity and spaciousness of the sound. In addition, no significant specular reflections should arrive at the mix position before or after the temporally diffuse reflections, since they would serve as competing sources and provide false directional clues. The diffuse reflections are lower in level and do not provide competing directional clues, but add intensity, body and ambience.

What is the optimum amplitude and phase or temporal distribution of the energy which we first psychoacoustically perceive returning to the mix position from the rear of the room? Consider the illustration of Figure 5. What is the effect of the three reflection patterns shown in the lower three histograms, on the steady state energy of the frequency illustrated. The steady state energy can be obtained by the coherent sum of the frequency shown, phase shifted by the intervals, ΔT , indicated. This is precisely the Fourier transform. For the equally spaced, equal energy reflection pattern at the bottom, the steady state energy is very nearly zero, for this frequency. The scattered energy will approach zero $(N-1)$ times between zero frequency and $c/N\Delta T$, where c is the velocity of sound. This generates a very non-uniform frequency response, which would not seem to be a particularly favorable reflection pattern to generate in the rear of the control room. The reflection pattern second from the bottom is generated from a quadratic-residue sequence ($n^2 \text{ mod } N$, where n ranges from 0 to infinity) with $N=19$ [5]. It can be seen that the Fourier transform of this sequence has constant energy at the frequency indicated and integral multiples thereof. At intermediate frequencies the energy is also approximately constant. The reflection pattern third from the bottom of Figure 5 is also a quadratic-residue sequence with $N=7$. The Fourier transform of this sequence also yields equal energy at this frequency and integral multiples and is approximately constant at intermediate frequencies. Surfaces treated with RPG diffusors based on quadratic-residue sequences have been found to provide early reflection patterns which temporally fuse with the direct sound in a psychoacoustically pleasing manner [5]. The lines in the histograms can also represent well depths in a quadratic-residue diffusor (QRD²). The more closely spaced depths of the QRD-19 provides better response at higher frequencies than the QRD-7, but the QRD-7 provides similar response at the frequency indicated with shallower wells. The width of the energy-time curve is essentially related to the depth of the deepest well in the sequence and the low frequency response. Hence we have chosen relatively deep wells to provide diffusion at low frequencies. The density of lines in the energy-time curve is related to the high frequency response. To provide uniform diffusion over more than four octaves we have utilized diffusors with a maximum depth of 16 inches, a well width of 1 inch, and a sequence with 43 wells per period. It is therefore apparent that the initial delay, amplitude and

temporal pattern of the initial sound returning to the mix position is important in coherent reinforcement of the stereo perspective provided by the direct sound and the temporal fusion of direct sound and diffuse early reflections.

The rear of the room consists of reflective and diffusive surfaces. The temporally and spatially diffuse energy is generated by one-dimensional RPG diffusors since they provide uniform broad-bandwidth wide-angle coverage, which is concentrated into a hemidisk. The reflective surfaces are positioned such that they do not reflect direct sound to the mix position, but rather, reflect direct sound to the diffuse surfaces. These surfaces then concentrate diffuse energy across the console. These reflective and diffusive surfaces are seen in the plan view of a control room in Figure 3. The earliest arriving diffuse energy (which is spread from 2-4 ms) at the mix position is from a speaker to the RPG on the same side (13.7 ms) and the latest arriving diffuse energy to the mix position is from the same speaker to the RPG on the opposite side (18.1 ms). These arrival times can easily be adjusted by positioning of the diffusors. The geometry of the rear half of the room and the orientation of RPGs and reflective surfaces essentially determine the energy versus time response after the latest directly arriving diffuse energy.

The elevation schematic of Figure 4 can be used to describe the vertical position of the RPGs for optimum energy concentration at the mix position. The angle of elevation to the high frequency speaker, α , and the distance from the high frequency speaker to the mix position, L_1 , are shown. L_1 is the projection of the distance from the speaker to the mix position, D . For an equilateral configuration, $L_1 = D \cos 30^\circ$. L_2 is the distance from the high frequency source to the mix position and L_3 is the distance from the mix position to the rear wall.

$$L_2 = L_1 \cos \alpha$$

The optimum vertical position of the RPG cluster on the rear wall is one which specularly directs the center of the diffuse scattered hemidisk back to the mix position. This ray is indicated with a solid line in Figure 4. The angle β is the angle the hemidisk makes with the diffusor normal the plane (long dash-dot) passing through the mix position. H_1 is the height of the high frequency source above the mix position, H_2 is the height of the center of the lower two laterally diffusing RPGs above the mix position and H_3 is the height of the mix position above the floor.

$$H_1 = L_1 \sin \alpha$$

$$\tan \beta = H_1 / (L_2 + 2L_3)$$

$$H_2 = L_3 \tan \beta$$

The energy-time curves (ETC), measured with the TEF analyzer, for two similar control rooms, with and without the RPGs on the rear wall are shown in Figure 6. In the upper curve the early energy arrives primarily from specular reflections which are centered at approximately

17 ms and 21 ms. The console reflection at 6 ms is also evident. The lower curve shows the temporal pattern when the RFG is used on the rear wall surfaces. Notice the highly diffuse reflections arriving after a reflection free initial time delay of approximately 17 ms. The diffuse sound field is free of significant specular reflections which could act as competing directional clues. The diffuse reflections do not compete as directional clues with the direct signal, but rather combine with the direct signal adding body and ambience. Because the energy is diffuse, the complex comb filtering is apatially uniform as opposed to the spatial dependence of specular reflections. Consequently, the stereo perspective is maintained across the entire width of the mixing console and in the rear of the room.

Figure 7 (top) shows a rear view of Acorn Sound Recorders, Hendersonville, Tennessee, designed by Bob Todrank of Valley Audio, Nashville, Tennessee. Figure 7 (middle) shows the A room of FTM Studios, Lakewood, Colorado and Figure 7 (bottom) shows a rear view of TRC Studios, Indianapolis, Indiana, both designed by Russell E. Berger II of Joiner-Pelton-Rose, Dallas, Texas.

4 ACKNOWLEDGEMENT

The authors would like to thank Neil Muncy for many helpful discussions regarding the RFZ.

5 REFERENCES

- [1] R.E. Berger II, "Speaker Boundary Interference Response (SBIR)", Synergetic Audio Concepts, Tech Topics, vol. 11, no. 5 (1984).
- [2] R.W. James, The Optical Principles of the Diffraction of X-Rays, vol. 2, Cornell University Press, Ithaca, New York (1965).
- [3] D. Davis and C. Davis, "The LEDE Concept for the Control of Acoustic and Psychoacoustic Parameters in Recording Control Rooms", J. Audio Eng. Soc., vol 28, no. 9, pp. 585-595 (September 1980).
- [4] L.L. Beranek, Music Acoustics and Architecture, Wiley, New York (1961).
- [5] P. D'Antonio and J.H. Konnert, "The Reflection Phase Grating Diffusor: Design Theory and Application", J. Audio Eng. Soc., vol. 32, no. 4, pp. 228-238 (April 1984).

FIGURE CAPTIONS:

Figure 1. A point source (dot) located near a trihedral corner ($x=y=z=0$) at coordinate (x,y,z) and the seven virtual sources created by reflections from the three boundary surfaces are shown. Three virtual sources (cross) arising from the $x=0$ and $y=0$ boundaries are in parentheses and the four virtual sources (circle) generated by the $z=0$ boundary are in square brackets.

Figure 2. The SBIR at three observation points with respect to a source (dot) located at $x=y=z=2$ feet from an orthogonal trihedral corner. The long-short dashed line represents the response observed at $(1.0, 8.66, 6.0)$ and the dashed line represents the $(5.0, 8.66, 6.0)$ position. Both observation positions indicated by crosses were calculated with the near-field approach of Eq. 1. The solid curve represents the SBIR for the far-field approach of Eq. 7. The near-field response indicates a positional dependence. The higher frequency interference effects are averaged in the integration over all possible orientations in the far-field response.

Figure 3. A plan view of a proposed LEDE design showing a front dead end (DE) which is characterized by an RFZ, created by a flush mounted speaker baffle and splayed absorber boundary surfaces. The RFZ is indicated by the region within the dashed lines. RPG diffusers are used to create the diffuse sound field required in the live end (LE). The RPGs are arranged to return energy passing the mix position after an initial time delay, over a broad time period and across the entire mixing console. The diffuse energy from the RPG is spread over 2-4 ms depending on the angle of incidence and the time between the earliest and latest arriving direct return from the diffusers is also in the vicinity of 4 ms.

Figure 4. An elevation view of a proposed LEDE design showing the splayed speaker baffle and inclined ceiling sections which create an RFZ above and behind the mix position.

Figure 5. (Top) This frequency and multiples of it are scattered uniformly by the quadratic-residue sequences illustrated in the second and third row of the figure. (second row) Quadratic-residue reflection pattern for prime number 19. (Third row) Quadratic-residue reflection pattern for prime number 7. (Bottom) Equally spaced, equal energy reflection pattern.

Figure 6. (Top) ETC for a LEDE control room having specularly reflective rear walls. (Bottom) ETC for a similar geometry with RPG diffusers on the rear walls.

Figure 7. (Top) Acorn Sound Recorders, Hendersonville, Tennessee, (middle) FTM Studios, Lakewood, Colorado, (Bottom) TRC Studios, Indianapolis, Indiana.

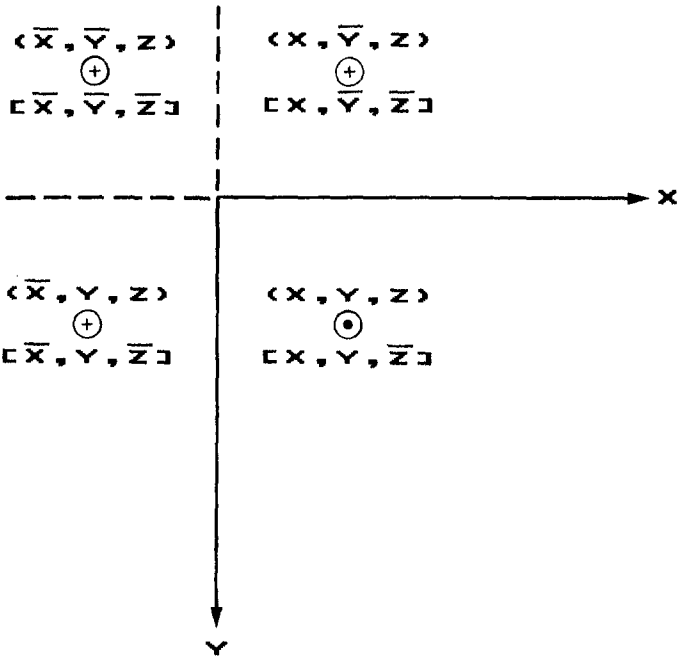


FIG. 1

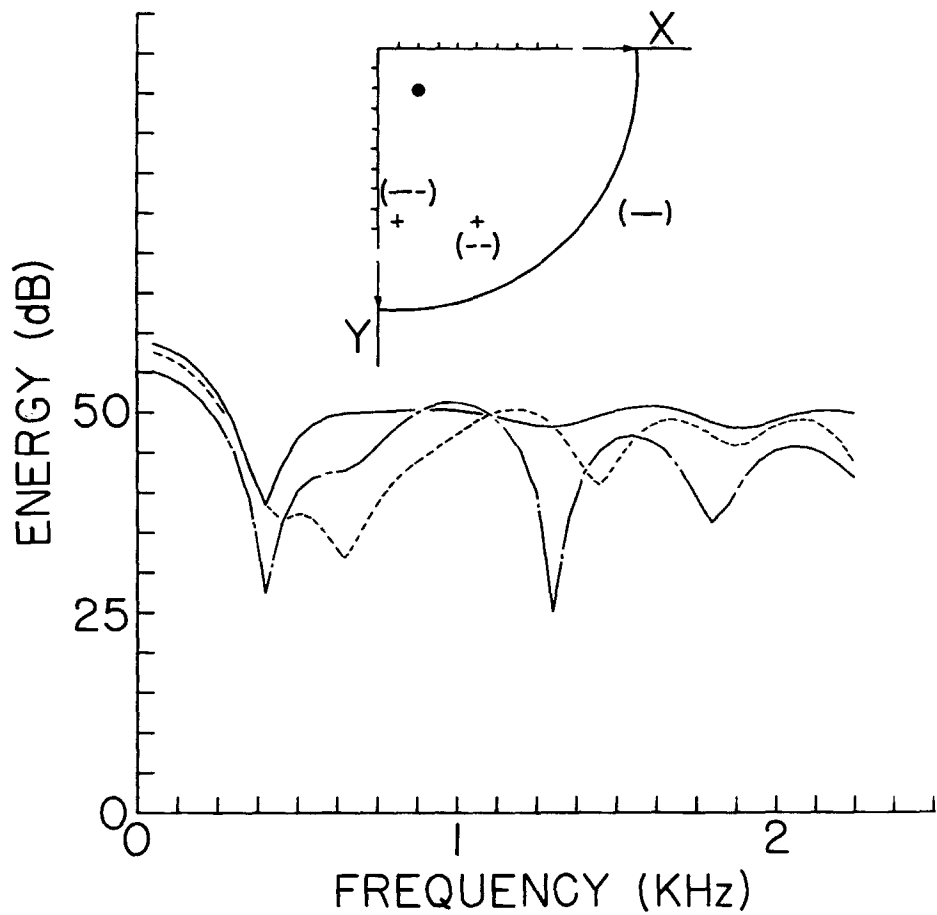


FIG. 2

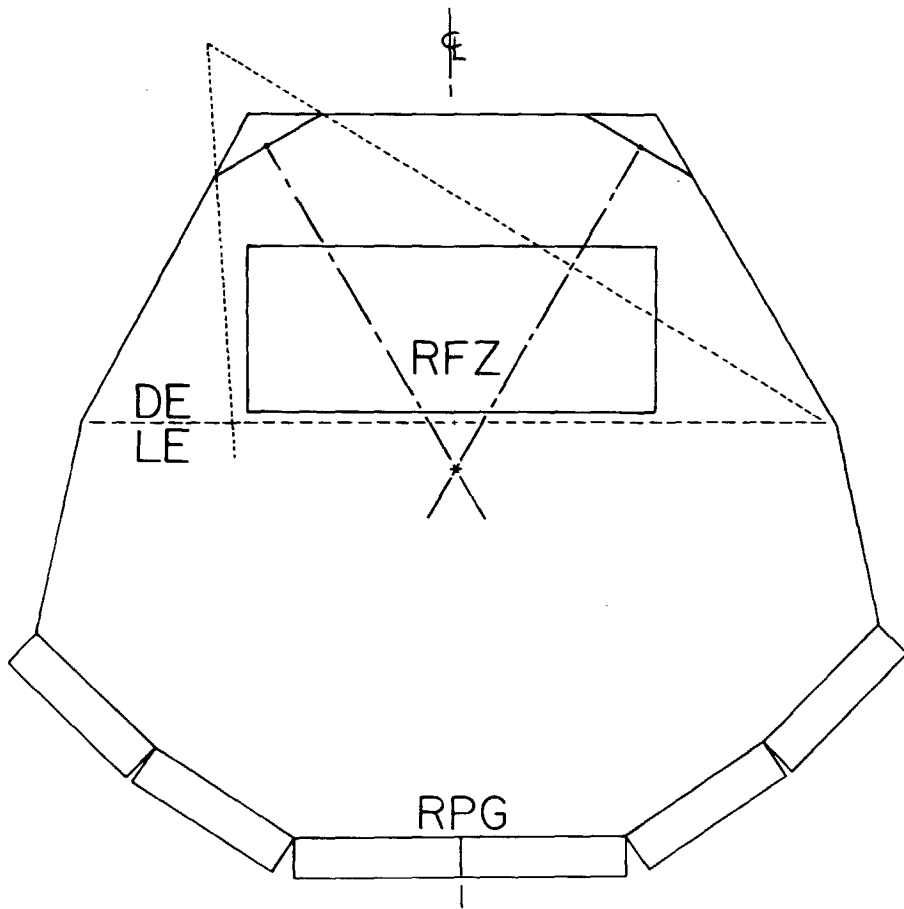


FIG. 3

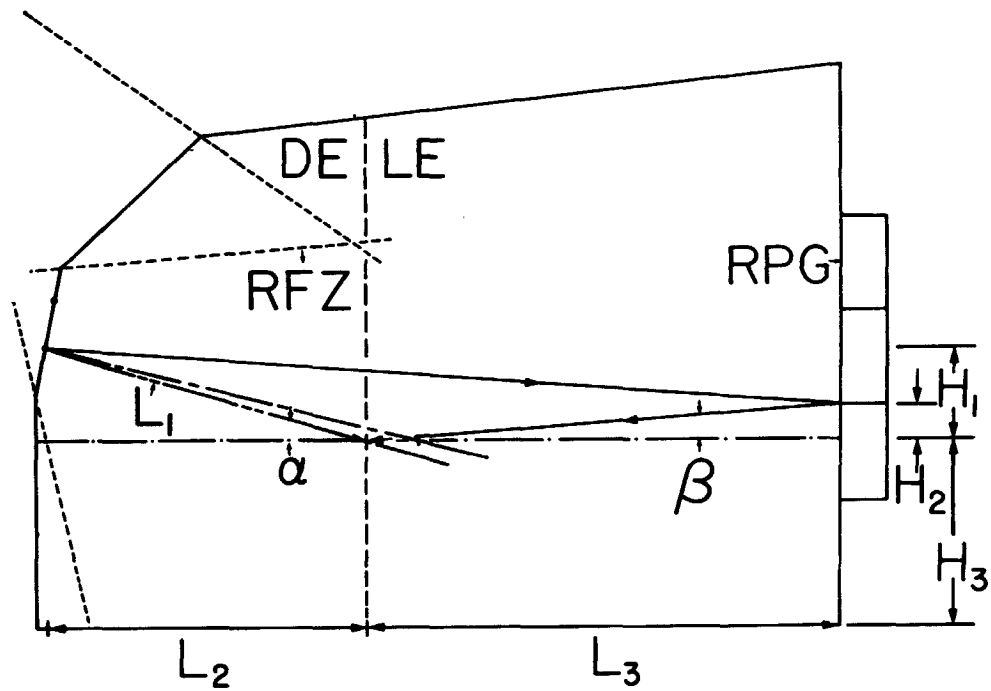


FIG. 4

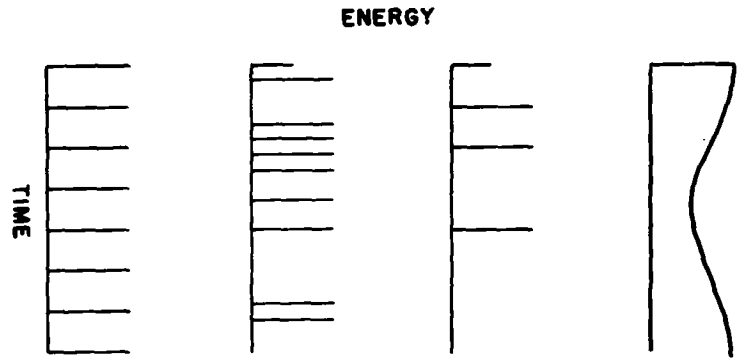


FIG. 5

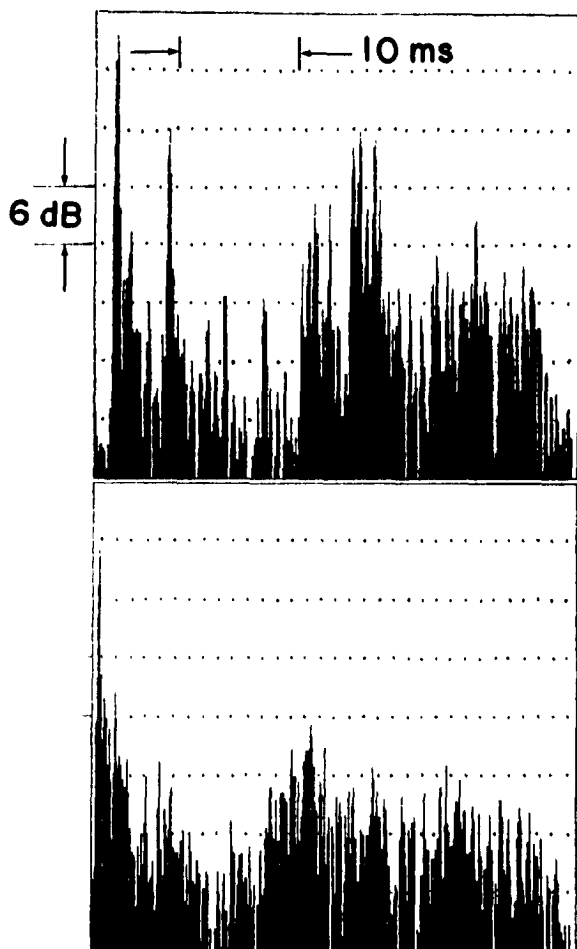


FIG. 6



FIG. 7(a)

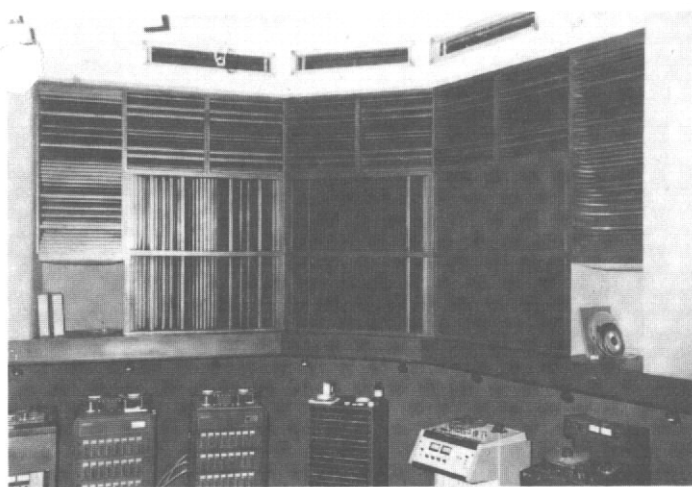


FIG. 7 (b)

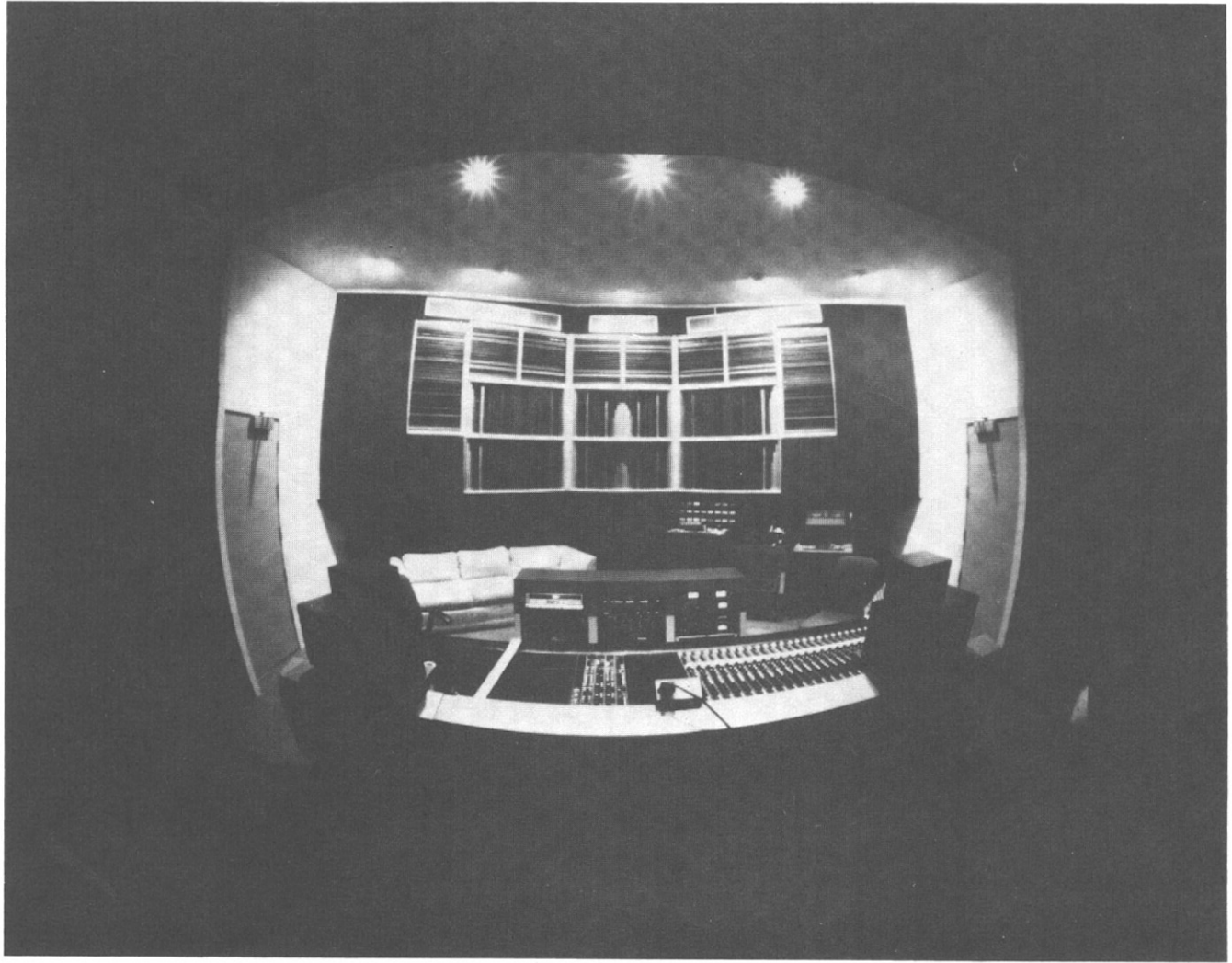


FIG. 7(c)